ARTICLE

# Highly basic solid catalysts obtained by spray drying of a $NaAlO_2$ and boehmite suspension for the upgrading of glycerol to acetins

Received 00th January 20xx,
Accepted 00th January 20xx

DOI: 10.1039/x0xx00000x

Sreerangappa Ramesh,[a] Makhlouf Amoura[b] and Damien P.Debecker[a]*

In here, we present the low-cost production of $NaAlO_2$-$Al_2O_3$ catalysts, which exhibit high activity in the transesterification of methyl acetate with glycerol to obtain acetins. The catalyst preparation procedure is based on the spray drying of a colloidal boehmite suspension, supplemented with a sodium aluminate ($NaAlO_2$) solution using a pilot scale spray drier. Upon subsequent calcination, we obtain spherical micro particles presenting a homogeneous dispersion of sodium aluminate and featuring high basicity. The $NaAlO_2$ loading has a marked impact on the basicity and textural properties of the final materials. These solids are found to be efficient heterogeneous base catalysts for the upgrading of glycerol (which is essentially a waste) to glycerol acetins (which are important bio-based fuel additives). With 100 mg of the catalyst loaded with 20 wt.% of $NaAlO_2$, a conversion of 96 % is obtained after 4 h of reaction at 60 °C (10 mmol of glycerol + 100 mmol of methyl acetate). Importantly, the selectivity for triacetin is as high as 20 % (the rest being 50 % of diacetin and 30 % of monoacetin). The catalysts act strictly in a heterogeneous way and are recyclable upon calcination.

## Introduction

Running liquid or gas phase reactions over a solid catalyst is the heart of modern energy, fuels and chemical production.[1, 2] Catalysis science plays a vital role in chemical industries, and most of the chemical process established commercially are performed with heterogeneous catalysts.[3] In the field of biodiesel production, for example, glycerol is formed as a by-product (accounting for ~10 wt.% of the biodiesel production) and must be upgraded to products of higher value in order to make the process economically viable.[4, 5] These upgrading reactions are typically operated with the help of heterogeneous catalysts,[6] to form dihydroxyacetone,[7] acrolein,[8] glycerol carbonate,[9-11] or synthesis gas.[12, 13] Recently the conversion of glycerol to glycerol acetins gained attention due to their high potential as fuel additives.[14] Acetins can be typically obtained either by esterification of acetic acid with glycerol in the presence of a solid acid catalyst[14-16] or by transesterification of an alkyl acetate with glycerol in the presence of a basic catalyst.[17]

Sodium aluminate ($NaAlO_2$) belongs to a class of super base solid materials; it finds diverse applications in paper industry, water treatment and as a precursor for zeolite synthesis.[18] With the idea to exploit the superior basic properties of sodium aluminate, it was recently tested as a heterogeneous catalyst for a range of base-catalysed organic transformations (transesterification, carboxymethylation, isomerization, condensation, etc.) and showed high catalytic performance.[19-25]

Yet, $NaAlO_2$ is highly corrosive and hygroscopic, which makes it difficult to use industrially. In the laboratory, the operator can notice this by the fact that glass wares are corroded when in contact with pure $NaAlO_2$ – difficult to clean after use. As it reacts with moisture, $NaAlO_2$ should be preserved in the desiccator. For these reasons, coating or supporting $NaAlO_2$ on a suitable carrier (e.g. on hydrotalcites[26] or titania[27], dolomite[28] and alumina[29]) was proposed as a pertinent strategy to produce highly basic and highly active heterogeneous catalysts that are easier to handle in the perspective of commercial applications. To deposit $NaAlO_2$ on a suitable support, simple impregnation methods can be applied, mixing a suspension of the preformed carrier with an aqueous $NaAlO_2$ solution, followed by evaporation, drying and calcination.

Moving further, we propose to carry out the deposition of sodium aluminate onto a carrier via spray drying. Aerosol processes encompass all procedures which involve the production of a gas-transported "mist" of liquid droplets which are further processed, typically by drying or thermal decomposition. As reviewed recently, the technical features of aerosol methods make them highly interesting for the production of tailored heterogeneous catalysts.[30] The method – heavily used for the preparation of industrial heterogeneous catalysts like for example cracking catalysts[31] – has the great advantage that it can be operated in a continuous mode and is relatively easily scaled up. The nature, composition and physico-chemical properties of the starting solution or suspension, together with the operating parameters of the spray drier will determine the properties of the final material, so that a wide range of divided materials with various size, shape, composition, and texture can be obtained.[32, 33] Thus, aerosol processes can be coupled with a flame

[a] *Institute of Condensed Matter and Nanosciences (IMCN), Université catholique de Louvain (UCLouvain), Place Louis Pasteur, 1, box L4.01.09, 1348 Louvain la-Neuve, Belgium. Email: damien.debecker@uclouvain.be*
[b] *Dequenne Chimie S.A, Route de Wallonie- Darse Nord, Ghlin, Belgium*

† Footnotes relating to the title and/or authors should appear here.
Electronic Supplementary Information (ESI) available: [details of any supplementary information available should be included here]. See DOI: 10.1039/x0xx00000x

technology to produce different types of non-porous nanomaterials and catalysts,[34] or with sol-gel chemistry to form a multitude of advanced catalysts including hierarchically porous metallosilicate catalysts,[35-37] hybrid catalysts,[38, 39] or even noble metal-based electrocatalysts.[40]

In this work, a pilot scale spray-dryer is used to coat a boehmite support with sodium aluminate, in one-pot, to obtain spherical microspheres which are then calcined to yield $NaAlO_2$-$Al_2O_3$ catalysts. The resulting materials are inspected in terms of basicity, texture, crystallinity, morphology, etc. Their high activity in the acetylation of glycerol with methyl acetate is discussed in the light of their physical and chemical properties.

## Results and discussion

Catalysts were prepared by the spray drying of a boehmite suspension, supplemented (or not) with a sodium aluminate solution. The reference materials was obtained in the absence of NaAlO2 and is denoted "B"; the sodium aluminate-boehmite mixtures are denoted "x SAB", where x is the nominal $NaAlO_2$ loading (in wt.%).

### Texture, morphology, crystallinity, and basicity

The morphology of the spray-dried catalysts was analysed by scanning electron microscope (SEM). The materials consists of spherical particles in the range 2 to 30 µm size range (the distribution is centred on 5 µm). Their spherical morphology is related to the preparation process in which particles are produced via the evaporation of the solvent (water) from spherical aerosol droplets. A similar morphology was observed for the catalysts obtained for B and SAB samples (see supplementary information, Fig. S1). The energy-dispersive X-ray (EDX) probe mounted on the SEM was used to map the different elements on 20 SAB (Fig. 1B). It appeared that $NaAlO_2$ was uniformly distributed throughout the sample (Fig. 1B).

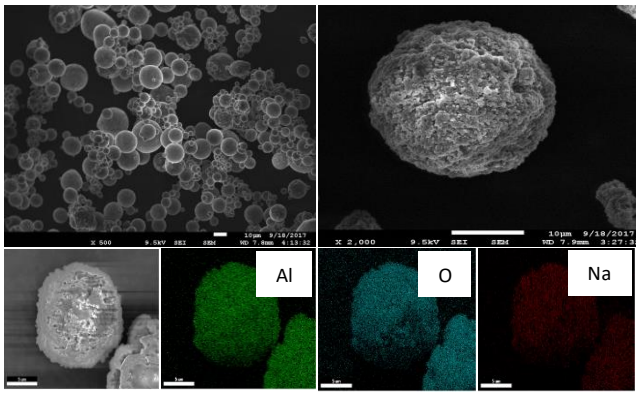


**Figure 1.** (top) SEM images of the 20SAB samples at different magnification values (other catalysts have been analysed in SEM too and showed similar morphologies – see electronic supplementary materials Fig. S1). (bottom) SEM-EDX elemental analysis on one microparticle of 20 SAB catalyst.

Pure sodium aluminate can be obtained commercially in the solid form, or by the drying of the sodium aluminate solution using vacuum drying or spray drying (here denoted "100 SA"). In both cases, these materials have a relatively very low specific surface area (SSA ~2.0 $m^2.g^{-1}$).[22] When spray drying the boehmite suspension alone, followed by calcination, the obtained alumina material (here denoted "B") shows high specific surface area (260 $m^2.g^{-1}$, see Table 1). Thus, sodium aluminate was incorporated in the solution before spray drying, targeting a loading of 5, 10 or 20 wt. % (5 SAB, 10 SAB and 20 SAB respectively). We choose to focus on a low $NaAlO_2$ loading range (5-20 wt.%) where we have observed that the powder could be manipulated easily (unlike pure $NaAlO_2$). After calcination, textural properties were drastically affected as compared to the pristine alumina obtained from boehmite. All catalysts showed $N_2$ physisorption isotherms of type IV according to IUPAC classification, characteristic of mesoporous materials (Fig. 2A). Yet, the total pore volume and the specific surface area dropped as the $NaAlO_2$ loading increased. For example, specific surface area drops from 260 $m^2.g^{-1}$ for the calcined boehmite (B) to 12 $m^2.g^{-1}$ for 20 SAB. Similar results were reported with hydrotalcite- and titania-based materials promoted by $NaAlO_2$.[27, 41]

**Table 1.** Textural properties of boehmite and $NaAlO_2$-promoted catalysts and amount of $CO_2$ detected in TPD.

| Catalyst | SSA ($m^2.g^{-1}$) | Pore volume ($cm^3/g$) | $CO_2$ adsorbed ($mmol_{CO2}/g$) |
|---|---|---|---|
| B | 260 | 0.65 | 0.05 |
| 5 SAB | 167 | 0.47 | 0.18 |
| 10 SAB | 92 | 0.26 | 0.32 |
| 20 SAB | 12 | 0.07 | 0.78 |
| $NaAlO_2$ | 2 | 0.01 | 0.80 |

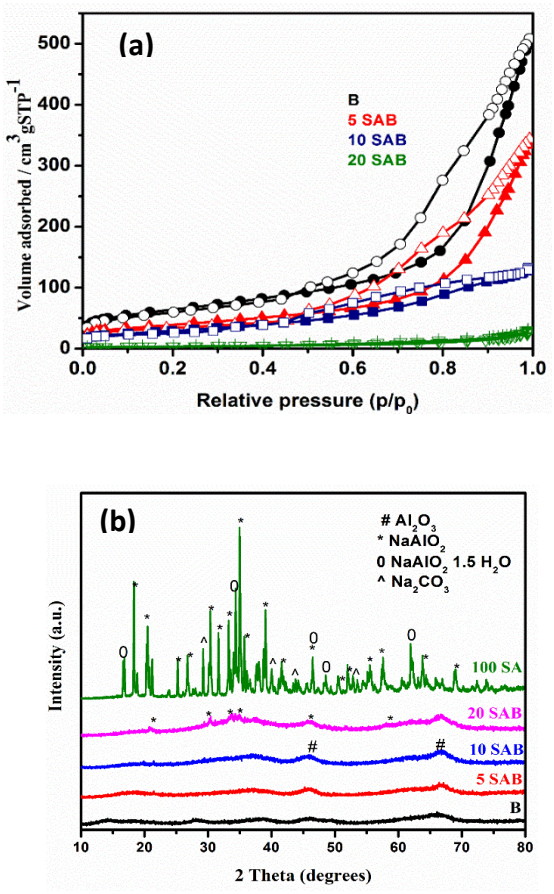


**Figure 2.** (a) Nitrogen adsorption (full symbols) and desorption (empty symbols) isotherms obtained on the catalysts prepared by spray drying and calcination. (b) Powder XRD patterns.

The crystallinity of the boehmite-based and sodium aluminate-promoted materials was examined by powder XRD (Fig 2b). The calcined boehmite gives weak and broad peaks corresponding to an γ-$Al_2O_3$ phase. Three crystalline phases are detected for sodium aluminate (aerosol made 100 SA): $NaAlO_2 \cdot 1.25H_2O$ (JCPDS 00-044-0430), $NaAlO_2$ (JCPDS 00-033-1200) and $Na_2CO_3$ (JCPDS 53-61386).[42, 43] In xSAB catalysts, at low sodium aluminate loading, no diffraction peaks is detected for sodium aluminate (for 5 and 10 wt % $NaAlO_2$) and only the broad patterns of alumina can be perceived. However, at 20 wt. % loading, characteristics peaks for sodium aluminate are observed. It is inferred that, at lower concentrations, $NaAlO_2$ is well distributed throughout the porous alumina matrix, while higher concentration leads to the formation of $NaAlO_2$ crystals possibly blocking the pores, consistent with the observed drastic decrease in surface area and pore volume in these materials.

The basicity of the prepared catalysts was approached by performing temperature programmed desorption of $CO_2$ (Fig. 3). The sample obtained by the spray drying of the boehmite suspensions (followed by calcination) showed only a small $CO_2$ desorption peak below 200 °C, demonstrating that it possesses only a low amount of weakly basic sites. On the contrary, pure $NaAlO_2$ shows two distinct desorption peaks at higher temperature. The desorption peak below 400 °C is generally considered as originating from weak basic sites and the desorption peak after 400 °C corresponding to strong basic sites.[44] It should be noted that sodium aluminate can react with $CO_2$ to form sodium carbonate, which will decompose only at high temperature. Thus, the integration of the $CO_2$ signal in TPD will give the amount of $CO_2$ that can be adsorbed in the chosen conditions for saturation and then desorbed under 750°C; this amount should not be referred to as a number of basic sites, but only as an indirect indication of the sample basicity.[27] Yet, clear trends can be observed here (Table 1). The addition of a small amount of $NaAlO_2$ to boehmite (5 SAB) results in a marked increase in the amount of $CO_2$ desorbed. The strength of basic sites appears to increase as well: the low temperature peak presents a "tail" at higher temperatures and an additional peak is detected at ~650 °C (Fig. 3). The basic strength increased progressively with the $NaAlO_2$ loading from 5 - 20 wt% as it can be seen on both the low and high temperature desorption peaks. Overall, in SAB catalysts, the basicity – both in terms of amount and strength – is found to increase with the $NaAlO_2$ loading.

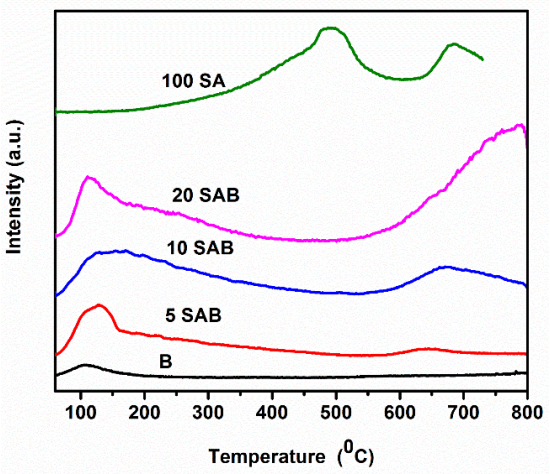


**Figure 3.** $CO_2$ TPD profiles obtained on the catalysts. The Y-axis has been re-scaled; only the shape of the profile should be considered here.

## Catalytic activity

When preformed in the absence of any catalyst, the transesterification of methyl acetate with glycerol proceeded only to a minor extent (4% glycerol conversion to monoacetin after 16h at 60°C). The boehmite also showed poor activity for acetins synthesis (6 % glycerol conversion after 16 h). On the contrary, pure sodium aluminate showed 57 % glycerol conversion in only 1 h. This is much higher as compared to other solid base catalysts such as MgO and hydrotalcites classically reported as catalysts for this reaction[45] and used here as benchmark catalysts (Table 2). This result is consistent with the fact that $NaAlO_2$ is a super base material and already showed high activity in other base-catalysed reactions. For all $NaAlO_2$-based catalysts, an apparent turnover frequency ("TOF") can be estimated, reaching around 100-150 $h^{-1}$, based on the glycerol conversion at 1h and on the number of active sites, as approached by TPD (Table S1).

**Table 2.** Conversion of glycerol to glycerol acetins with different catalysts

| Catalyst | Glycerol conversion (%)[a] | Selectivity (%) | | |
|---|---|---|---|---|
| | | Mono | Di | Tri |
| Blank | 4[b] | 100 | -- | -- |
| B | 6[b] | 100 | -- | -- |
| 5 SAB | 30 | 71 | 27 | 2 |
| 10 SAB | 43 | 66 | 31 | 3 |
| 20 SAB | 62 | 57 | 38 | 5 |
| $NaAlO_2$ | 57 | 58 | 37 | 5 |
| MgO | 37 | 80 | 19 | 1 |
| Hydrotalcites | 45 | 71 | 27 | 2 |

[a]Reaction conditions: 0.10 g of catalyst, mole ratio of 1:10 (Gly: MA) at 60°C for 1h.
[b]Same reaction conditions, but maintained for 16h.

Adding only 5 wt.% of $NaAlO_2$ to the inactive boehmite-based material allowed to reach 30% glycerol conversion in only 1h (5 SAB, Table 2). This level of activity further increases with increasing the $NaAlO_2$ loading. The boost in catalytic activity is directly related with the enhanced basicity strength brought about by $NaAlO_2$. The boehmite loaded with 20 wt.% of $NaAlO_2$ (20 SAB) is the most active sample in this study.

Interestingly, it also showed relatively high selectivity for triacetin (5 % in 1 h). This is higher than the values typically reported on this reaction.[45] The direct formation of significant amounts of triacetin may tentatively be attributed to the presence of strong basic sites in $NaAlO_2$-based materials (yields and carbon balance are reported in Table S2). This is notable because the latter triacetin has a much higher value, as fuel additives, as compared to mono acetin (and diacetins). In fact, a correlation can be established between the amount of $CO_2$ detected in TPD (related to basicity) and the intrinsic activity of the catalysts (Fig. S2).

A full kinetic profile was obtained for 20 SAB (Fig. 4a). As expected, glycerol conversion continued to increase up to 96 % after 4 h reaction time. With time the selectivity to di- and triacetins

increased at the expense of mono acetin. After 4h of reaction, around 50% selectivity for diacetins and 20 % selectivity for triacetin was observed. However, after 4h of reaction, the system seemed to reach a plateau, indicating a probable catalyst deactivation (see below). At this stage, a turnover number (TON) of 123 can be calculated (Table S1).

Besides the good catalytic activity, stability and reusability are also important factors to be considered. To investigate the heterogeneous nature of the SAB catalysts, a hot filtration test was conducted. After 1 h of reaction, 10 mL of ethanol was added to dissolve all reactants and product and obtain a single phase. The reaction mixture was filtered off to remove the solid; the resulting mixture was evaporated in the rotavapor to remove ethanol. Fresh MA (7.4 g) was added and it was refluxed (60 °C) for an additional 3 h. Analysis of the final reaction mixture showed no further glycerol conversion or increase in selectivity for di or tri acetins, which clearly demonstrated that no active species is leaching into the solution (Fig. 4b).

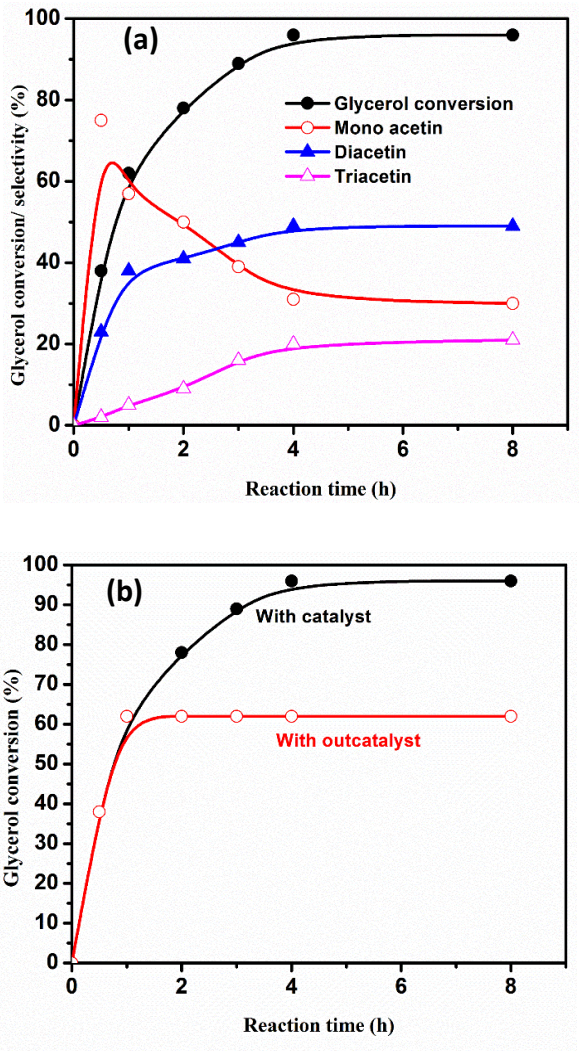


**Figure 4.** (a) Effect of reaction time on glycerol conversion and acetins selectivity. Reaction conditions: 10 mmol of glycerol, 100 mmol of methyl acetate with 0.100 g of 20 SAB at 60 °C. (b) hot filtration test carried out in the same conditions, but removing the catalyst (red line, empty symbols) after 1 h and continuing the reaction for an additional 3 h.

To further confirm the reusability of the catalyst, recycling tests were performed. After the desired reaction time (1 h), the reaction mixture was cooled down to room temperature, diluted with 10 mL ethanol, and the solid catalyst was separated by filtration. The catalyst was further washed three times with ethanol (5 mL), and then it was dried at 120 °C in an oven for 4 h followed by calcination at 400 °C for 4 h and used with fresh reactants. After this treatment, the catalyst showed the same activity (both glycerol conversion and acetins selectivity) as that of the fresh catalyst (Fig. 5). It must be noted that the spent catalyst is totally inactive if the calcination step is omitted after recovery. So what we call "reusability" should only be understood as "reusability after proper reactivation". On an applied perspective, this constitutes a clear limitation of these catalysts. On a fundamental level, it clearly points to a deactivation by poisoning (strong adsorption of organic species on the active sites).

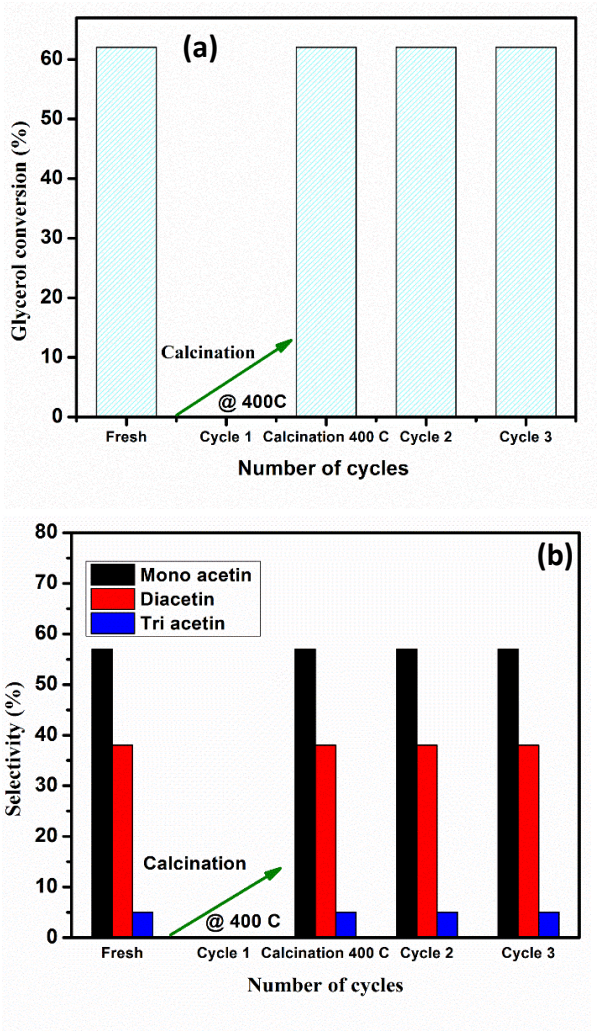


**Figure 5.** Reusability studies. (a) Glycerol conversion after several rounds of recycling (with reactivation by calcination). (b) Acetins selectivity during these recycling tests. Reaction conditions: 10 mmol of glycerol, 100 mmol of methyl acetate with 0.100 g of 20 SAB at 60 °C for 1 h, after that catalyst was filtered, washed with ethanol and calcined at 400 °C for 4h before used for next cycle.

## Conclusions

Novel solid base heterogeneous catalysts were produced by promoting a boehmite materials with sodium aluminate, in one-step using a pilot scale spray-drier. Upon calcination, $NaAlO_2$-promoted alumina-based catalysts are obtained which feature strong basic properties that can be tuned by controlling the loading of sodium aluminate. These catalysts are obtained easily, in a continuous mode and from inexpensive starting materials. As compared to the pristine boehmite support, the textural properties of the promoted materials are strongly affected by the presence of sodium aluminate. Yet the catalysts showed excellent activity for the base-catalysed transesterification of methyl acetate with glycerol, outcompeting conventional basic catalysts. We report relatively high selectivity for triacetin (up to 20%). The catalysts behave strictly in a heterogeneous mode, and can be recycled upon calcination. Thus, we propose these materials as suitable industrial basic catalysts, which may also find potential applications in other base-catalysed reactions.

## Experimental

The sodium aluminate aqueous solution (23 wt. %) and the water dispersible boehmite were kindly provided by respectively Dequachim and Dequenne chimie (Belgium). Glycerol (99 %) and methyl acetate (99.5 %) were obtained from Sigma Aldrich Belgium and used as received. Ethanol (99 %) was obtained from VWR. Mono acetin (40.0 %) (TCI), di acetin (50.0 %) and tri acetin (99.0%) (Fluka) were used as standards for GC calibration.

### Catalyst preparation

Boehmite-supported $NaAlO_2$ was synthesized in a pilot scale industrial spray drier (ANHYDRO compact spray Dryer-type 3.58.50.01). The required quantity of sodium aluminate solution (0, 25, 50 and 100 mL) was diluted with 4L distilled water, and then 500 mL of boehmite colloidal suspension (25 wt. %) was added slowly. The mixture was stirred at room temperature for about 2 h using a mechanical stirrer (500 RPM). The resulting suspension was atomized and dried in a cyclone drier. The spray dryer was equipped with a centrifugal atomizer (disc diameter: 100mm) and used ate an atomizing velocity of 25000 rpm. The product was spray-dried at an inlet air temperature of 300 °C and an outlet air temperature of 125 °C. The water evaporation rate of the dryer was 28 $kg.h^{-1}$. The resulting materials were calcined at 550°C for 4 h in air in a muffle furnace before being used for further studies. Catalysts are denoted xSAB (x = $NaAlO_2$ wt. % nominal loading, SA = sodium aluminate, B = boehmite). For the comparison, 100 SA prepared by spray drying sodium aluminate solution and the detailed procedure is reported in the supporting information.

### Catalyst characterization

X-ray diffraction (XRD) powder patterns were collected on a Siemens diffractometer model D5000 fitted with a Cu Kα (1.541°) radiation source. Data were recorded over a 2θ range of 10–80° with an angular step of 0.05° at 3 s/step which resulted in a scan rate of 1°/min. Textural properties were determined by nitrogen physisorption at 77 K using a Micromeritics Tristar equipment. Samples were previously degassed overnight at 393 K under vacuum. $CO_2$ temperature-programmed desorption (TPD) experiments were conducted using a CATLAB instrument from Hiden, equipped with QGA mass spectrometer for gas analysis. Approximately 80 mg of each sample was loaded in a quartz micro-reactor supported by quartz wool and degassed at 500 °C for 1h using a heating rate of 10 °C/min in flowing helium (50 $cm^3min^{-1}$). Next, the samples were cooled to 50 °C and exposed to flowing 15 % $CO_2$-Ar (50 $cm^3min^{-1}$) for 1.5 h and finally purged in flowing helium for 3h at 50°C. In the TPD experiments, the sample was heated up to 750°C or 800°C using a heating rate of 5 °C $min^{-1}$ and a He flow of 50 $cm^3min^{-1}$. The total amount of desorbed $CO_2$ was obtained by integration of the desorption profiles (up to 750°C) and referenced to the signals calibrated for known volumes of analyzed gases. Scanning Electron Microscope (SEM) images were used to determine the morphology of the studied samples. SEM images were taken with a JEOL 7600 F with a 15.0 kV voltage. Samples were dried under vacuum at 60 °C for 24 h and then placed on a piece of carbon black tape on an aluminium stub. A chromium sputter coating of 10 nm was applied under vacuum with a Sputter Metal 208 HR (Cressington).

### Glycerol acetins synthesis

Transesterification of methyl acetate with glycerol was carried out in an oven-dried 25 mL round-bottom flask fitted with a water-cooled condenser. The reaction was initiated by introducing 10 mmol of glycerol (0.92 g), 100 mmol of methyl acetate (7.4 g), 0.2 g of dimethyl formamide (DMF, as the internal standard) and the catalyst (100 mg, oven dried at 120°C for 30 min before being used in the reaction). Then, the reaction mixture was brought to 60 °C in an oil batch and allowed to react for 0 to 8 h, under stirring (500 RPM). After the reaction, the mixture was allowed to cool down to room temperature, and dissolved in 10.0 g of ethanol for GC analysis.

The reaction products were analysed by gas chromatography on a GC-456 from Scion Bruker equipped with a flame ionization detector, split/split less injection unit and a capillary column (DB-WAX, 30 m, 0.25 mm, 0.25 m). Helium was used as the carrier gas. The injection (5 µl) was performed in split mode with a split ratio of 100:1. Initially, the oven temperature was set at 100 °C and then increased at the rate of 15 °C.$min^{-1}$ until it reached 240 °C and then it was maintained at this temperature for 15 min. The FID and injection temperatures were fixed at 270 °C and 300 °C, respectively.

## Conflicts of interest

There are no conflicts to declare

## Acknowledgements

Authors gratefully acknowledge the Walloon Region for the financial support (BEWARE programme, convention n° 1410279). Dr. F. Devred is thanked for the logistical and technical help.

## Notes and references


1. P. Munnik, P. E. de Jongh and K. P. de Jong, *Chemical Reviews*, 2015, **115**, 6687.
2. R. Schlögl, *Angew. Chem. Int. Ed.*, 2015, **54**, 3465.
3. S. M. George, *Chemical Reviews*, 1995, **95**, 475.
4. N. J. Venkatesha and S. Ramesh, *Industrial & Engineering Chemistry Research*, 2018, **57**, 1506.
5. M. Pagliaro, R. Ciriminna, H. Kimura, M. Rossi and C. Della Pina, 2007, **46**, 4434.
6. M. Pagliaro, R. Ciriminna, H. Kimura, M. Rossi and C. Della Pina, *Angew. Chem. Int. Ed.*, 2007, **46**, 4434.
7. S. Hirasawa, Y. Nakagawa and K. Tomishige, *Catalysis Science & Technology*, 2012, **2**, 1150.
8. A. Ulgen and W. F. Hoelderich, *Applied Catalysis A: General*, 2011, **400**, 34.
9. W. K. Teng, G. C. Ngoh, R. Yusoff and M. K. Aroua, *Energy Conversion and Management*, 2014, **88**, 484.
10. M. O. Sonnati, S. Amigoni, E. P. Taffin de Givenchy, T. Darmanin, O. Choulet and F. Guittard, *Green Chem.*, 2013, **15**, 283.
11. P. de Caro, M. Bandres, M. Urrutigoïty, C. Cecutti and S. Thiebaud-Roux, *Front Chem*, 2019, **7**, 308.
12. S. Ramesh, E.-H. Yang, J.-S. Jung and D. J. Moon, *International Journal of Hydrogen Energy*, 2015, **40**, 11428.
13. S. Ramesh and N. J. Venkatesha, *ACS Sustainable Chemistry & Engineering*, 2017, **5**, 1339.
14. S. Veluturla, A. Narula, S. R. D and S. P. Shetty, *Resource-Efficient Technologies*, 2017, **3**, 337.
15. M. Aghbashlo, M. Tabatabaei, H. Rastegari and H. S. Ghaziaskar, *Journal of Cleaner Production*, 2018, **183**, 1265.
16. H. Rastegari, H. S. Ghaziaskar and M. Yalpani, *Industrial & Engineering Chemistry Research*, 2015, **54**, 3279.
17. S. Sandesh, P. K. R. Kristachar, P. Manjunathan, A. B. Halgeri and G. V. Shanbhag, *Applied Catalysis A: General*, 2016, **523**, 1.
18. T. Wan, P. Yu, S. Wang and Y. Luo, *Energy & Fuels*, 2009, **23**, 1089.
19. S. Ramesh and D. P. Debecker, *Catal. Commun.*, 2017, **97**, 102.
20. S. K. Cherikkallinmel, A. Gopalakrishnan, Z. Yaakob, R. M. Ramakrishnan, S. Sugunan and B. N. Narayanan, *RSC Advances*, 2015, **5**, 46290.
21. S. Lou, L. Jia, X. Guo, W. Wu, L. Gao, H. Wu and J. Wang, *RSC Adv.*, 2016, **6**, 6921.
22. S. Ramesh, K. Indukuri, O. Riant and D. P. Debecker, *Organic Process Research & Development*, 2018, **22**, 1846.
23. S. Despax, B. Estrine, N. Hoffmann, J. Le Bras, S. Marinkovic and J. Muzart, *Catal. Commun.*, 2013, **39**, 35.
24. M. Wang, M. A. A. Gasmalla, H. Admassu Tessema, X. Hua and R. Yang, *Food Chem.*, 2017, **233**, 151.
25. S. Ramesh, F. Devred and D. P. Debecker, *ChemistrySelect*, 2020, **5**, 300.
26. S. Ramesh, L. van den Biggelaar, F. Devred and D. P. Debecker, *ChemCatChem*, 2018, **10**, 1398.
27. S. Ramesh, F. Devred and D. P. Debecker, *Appl. Catal. A*, 2019, **581**, 31.
28. Y. Ning, S. Niu, S. Zhao, X. Zhang, Y. Zhang, K. Han, C. Lu and X. Zhang, 2019, **4**, 9849.
29. Y. Zhang, S. Niu, C. Lu, Z. Gong and X. Hu, *Energy Conversion and Management*, 2019, DOI: https://doi.org/10.1016/j.enconman.2019.112263, 112263.
30. D. P. Debecker, S. Le Bras, C. Boissière, A. Chaumonnot and C. Sanchez, *Chem. Soc. Rev.*, 2018, **47**, 4112.
31. S. Aghamohammadi and M. Haghighi, *Applied Clay Science*, 2019, **170**, 70.
32. A. B. D. Nandiyanto and K. Okuyama, *Adv. Powder Technol.*, 2011, **22**, 1.
33. C. Boissiere, D. Grosso, A. Chaumonnot, L. Nicole and C. Sanchez, *Adv. Mater.*, 2011, **23**, 599.
34. R. Koirala, S. E. Pratsinis and A. Baiker, *Chem. Soc. Rev.*, 2016, **45**, 3053.
35. V. Smeets, C. Boissière, C. Sanchez, E. M. Gaigneaux, E. Peeters, B. F. Sels, M. Dusselier and D. P. Debecker, *Chem. Mater.*, 2019, **31**, 1610.
36. G. Xiong, M. Feng, J. Liu, Q. Meng, L. Liu and H. Guo, *RSC Adv.*, 2019, **9**, 3653.
37. D. P. Debecker, M. Stoyanova, U. Rodemerck, F. Colbeau-Justin, C. Boissère, A. Chaumonnot, A. Bonduelle and C. Sanchez, *Appl. Catal. A*, 2014, **470**, 458.
38. A. Vivian, L. Fusaro, D. P. Debecker and C. Aprile, *ACS Sus. Chem. Eng.*, 2018, **6**, 14095.
39. N. Gholampour, S. Chaemchuen, Z.-Y. Hu, B. Mousavi, G. Van Tendeloo and F. Verpoort, *Chem. Eng. J.*, 2017, **322**, 702.
40. M. Faustini, M. Giraud, D. Jones, J. Rozière, M. Dupont, T. R. Porter, S. Nowak, M. Bahri, O. Ersen, C. Sanchez, C. Boissière, C. Tard and J. Peron, *Advanced Energy Materials*, 2019, **9**, 1802136.
41. S. Ramesh, F. Devred, L. van den Biggelaar and D. P. Debecker, 2018, **10**, 1398.
42. A. P. de Kroon, G. W. Schäfer and F. Aldinger, *J. Alloys Compd.*, 2001, **314**, 147.
43. J. A. Kaduk and S. Pei, *J. Solid State Chem.*, 1995, **115**, 126.
44. X. Yu, N. Wang, W. Chu and M. Liu, *Chemical Engineering Journal*, 2012, **209**, 623.
45. U. I. Nda-Umar, I. Ramli, Y. H. Taufiq-Yap and E. N. Muhamad, *Catalysts*, 2018, **9**, 15.


1